

THE HISTORY OF THE MYSTERIOUS ECLIPSES OF KH 15D
II. ASIAGO, KISO, KITT PEAK, MT. WILSON,
PALOMAR, TAUTENBURG AND ROZHEN OBSERVATORIES, 1954-97

JOHN ASHER JOHNSON¹, JOSHUA N. WINN^{2,3}, FRANCESCA RAMPAZZI⁴, CESARE BARBIERI⁴, HIROYUKI MITO⁵, KEN-ICHI TARUSAWA⁵, MILCHO TSVETKOV^{6,7}, ANA BORISOVA⁷, HELMUT MEUSINGER⁸

Draft version November 7, 2018

ABSTRACT

The unusual pre-main-sequence binary star named KH 15D undergoes remarkably deep and long-lasting periodic eclipses. Some clues about the reason for these eclipses have come from the observed evolution of the system's light curve over the last century. Here we present *UBVRI* photometry of KH 15D based on photographic plates from various observatories, ranging in time from 1954 to 1997. The system has been variable at the ≈ 1 mag level since at least 1965. There is no evidence for color variations, with a typical limit of $\Delta(B - V) < 0.2$ mag. We confirm some previously published results that were based on a smaller sample of plates: from approximately 1965 to 1990, the total flux was modulated with the 48-day orbital period of the binary, but the maximum flux was larger, the fractional variations were smaller, and the phase of minimum flux was shifted by almost a half-cycle relative to the modern light curve. All these results are consistent with the recently proposed theory that KH 15D is being occulted by an inclined, precessing, circumbinary ring.

Subject headings: stars: pre-main sequence — stars: individual (KH 15D) — circumstellar matter — techniques: photometric

1. INTRODUCTION

The T Tauri star known as KH 15D (Kearns & Herbst 1998) called attention to itself through a remarkable pattern of photometric variations. Every 48 days, the system dims by over 3 magnitudes (Hamilton et al. 2001; Herbst et al. 2002). It remains in this faint state for a duration that has grown from about 16 days in 1997, when the periodicity of the variations was first noticed, to over 24 days in 2004. Before 1999, the faint state was characterized by a short interruption of about 5 days during which the system returned to its bright state. Since then, these “rebrightening” events have subsided to near-undetectability.

Hamilton et al. (2001) and Herbst et al. (2002) argued persuasively that these dramatic and unusual variations are due to eclipses by circumstellar dust that surrounds the visible K7 star, although the arrangement of the dust and the cause of the periodicity were unknown. At the time, it was not even clear whether the system was a single star or a multiple star system, and hence whether the relative velocity of the dusty structure and the visible star was due to the orbital motion of the dust, or of the star (Herbst et al. 2002). The mystery of the eclipses

of KH 15D motivated an intensive monitoring campaign by observers around the world (Herbst et al. 2002; Barsunova et al. 2004), attracted other observers seeking clues in deep imaging (Tokunaga et al. 2004) and spectroscopy (Agol et al. 2004; Deming et al. 2004), and also attracted theorists hoping to model the circumstellar environment (Barge & Viton 2003; Grinin & Tambovtseva 2002).

An important step in the clarification of the basic system properties was the analysis of archival photographic plates of NGC 2264, the 3 Myr old star cluster in which KH 15D resides. Photographs from years prior to 1951 showed no evidence of eclipses deeper than 1 mag (Winn et al. 2003). More interestingly, photometry from 1967–1982 (Johnson & Winn 2004, hereafter Paper I) showed that eclipses were occurring with the same 48-day period as today, but with three striking differences: the system was brighter at all phases, the fractional variations in the total light were smaller, and the phase of minimum light was shifted relative to the modern light curve.

Motivated by these findings, Winn et al. (2004) proposed that KH 15D is a binary star that is gradually being occulted by an opaque foreground screen, which is probably the edge of an inclined, precessing, circumbinary disk. Chiang & Murray-Clay (2004) had the same idea independently, and explored the dynamical issues further, arguing that the “disk” was likely to be a fairly narrow ring. A radial velocity study by Johnson et al. (2004) confirmed that KH 15D is a binary star, and to the extent that the orbital parameters of the binary could be constrained by the radial velocities, the orbital parameters agreed well with the predictions of Winn et al. (2004). These developments have made KH 15D less mysterious than it once was, and they bring closer to reality the prospect of using the system to learn about disk evolution, the circumstellar environment of young stars,

¹ Department of Astronomy, University of California, Mail Code 3411, Berkeley, CA 94720

² Harvard-Smithsonian Center for Astrophysics, 60 Garden St., Cambridge, MA 02138

³ Hubble Fellow

⁴ Department of Astronomy, University of Padova, Vicolo Osservatorio 2, 35122 Padova Italy

⁵ Kiso Observatory, Institute of Astronomy, School of Science, University of Tokyo, Mitake-mura, Kiso-gun, Nagano-ken, 397-0101, Japan

⁶ Institute of Astronomy, Bulgarian Academy of Sciences; Tsarigradsko Shosse Blvd. 72, Sofia-1784, Bulgaria

⁷ Space Research Institute, Bulgarian Academy of Sciences, Moskovska Str. 6, Sofia-1000, Bulgaria

⁸ Thüringer Landessternwarte Tautenburg, Sternwarte 5, D-07778 Tautenburg, Germany

and possibly even planet formation.

A prerequisite for a complete model of the binary orbit and the surrounding disk or ring is a light curve with reasonably complete time and phase coverage over the entire era of the periodic variations. Towards that end, we present additional photometry of KH 15D based on an analysis of photographic plates from several archives around the world, ranging in time from 1954 to 1997, with most of the data coming from years prior to 1985. Our plate selection and digitization process are described in § 2, and the photometric measurements and uncertainties are described in § 3. In § 4, we present the light curves and describe the evolution that have been observed over the past 50 years. In § 5 we discuss these findings in the context of our model of the system.

2. THE PLATES

In Paper I, we presented results from an analysis of 52 photographic plates in the archive of the Astrophysical Observatory of Asiago, in northern Italy. All of those plates were derived from observations with a single telescope, the 67/92 cm Schmidt telescope, and almost all of them were exposed with a red filter (RG5, or equivalently RG665) and a red-sensitive emulsion (I-N). We deliberately selected this subset of plates for the first phase of our archival study of KH 15D, because they formed a fairly dense time series with uniform characteristics, and because the effective band pass was approximately the same as the Cousins *I* band, in which most of the modern CCD-based photometry has been obtained. In addition, the photometry was simplified for the I-N/RG5 plates because the glare from a nearby B star is much smaller on red-sensitive plates than it is on the more commonly used blue-sensitive plates.

Now that our photometric procedure has been tested thoroughly, we have expanded our analysis to include a heterogeneous collection of plates, obtained with different telescopes and effective band passes. The sample of 87 plates that is considered in this paper is drawn from the following sources⁹:

1. There are 26 plates from Asiago Observatory, the same archive from which the sample in Paper I was drawn (Barbieri et al. 2003). But whereas the previously analyzed plates were taken with the 67/92 cm Schmidt telescope, the plates in the present sample were taken with the 40/50 cm Schmidt telescope and the 1.22 m Galilei telescope. As in Paper I, these plates were digitized at Asiago Observatory with a 1600 dpi, 14-bit commercial flatbed scanner.
2. There are 35 plates that were taken with the 105/150 cm Schmidt telescope at Kiso Observatory, in Japan, a facility of the University of Tokyo. The Kiso plates were digitized at the observatory with a PDS microdensitometer.
3. There are 7 plates that were taken with the 134/200 cm Schmidt telescope of the Thüringer Landessternwarte Tautenburg, which is located

near Jena, in Germany. They were digitized using the local high-precision plate scanner TPS at 2540 dpi and 12 bits pixel⁻¹. (Brunzendorf & Meusinger 1999).

4. There are 7 plates that were taken with the 4 m Mayall telescope at Kitt Peak National Observatory, which is located near Tucson, Arizona. The plates were shipped to the Harvard College Observatory for digitization with a 1600 dpi, 14 bits pixel⁻¹ commercial flatbed scanner.
5. There are 5 plates taken with the 60 inch telescope of Mount Wilson Observatory, in the San Gabriel mountains of California, which were also shipped to the Harvard College Observatory for scanning.
6. There are 4 plates that were taken with the 2 m Ritchey-Chretien-Coude (RCC) telescope at the National Astronomical Observatory in Rozhen, Bulgaria. These plates were scanned with a 1600 dpi, 14 bits pixel⁻¹ scanner that is similar to the one used at Asiago Observatory.
7. Finally, there are 3 plates from the Palomar Observatory Sky Survey obtained with the 122/183 cm Oschin Schmidt telescope. These were scanned using the USNO PMM plate scanner. The digitized images were downloaded from the Space Telescope Science Institute web site¹⁰.

3. PHOTOMETRY

The scanning process produces a digital record of the density of opaque grains in the photographic emulsion as a function of the position on the plate. As in Paper I, we used a form of profile photometry (also known as point-spread-function, or PSF, photometry) in order to estimate the apparent magnitude of KH 15D on each plate, relative to a grid of local reference stars. This procedure is described fully in Paper I and is summarized below.

The relationship between the density enhancement, $d(x, y)$, and the flux received from the star, S , is nonlinear, and for bright stars the density saturates at a maximum value. Thus, an accurate PSF model must include a nonlinear response. We employed the model described by Stetson (1979), in which the PSF model is a magnitude-dependent transformation of a two-dimensional Gaussian distribution,

$$d_S(x, y) = [d_G(x, y)^{-q} + d_{\text{sat}}^{-q}]^{-1/q}, \quad (1)$$

where d_{sat} and q describe the saturation properties of the plate, and $d_G(x, y)$ is a Gaussian function of the coordinates x and y . The Stetson function has the desirable limits $d_S \rightarrow d_G$ for $d_G \ll d_{\text{sat}}$, and $d_S \rightarrow d_{\text{sat}}$ for $d_G \gg d_{\text{sat}}$.

The model is fitted to the stellar image using a nonlinear least-squares algorithm, and S is computed as the two-dimensional integral of $d_G(x, y)$. This flux scale is related to a standard magnitude via the expression

$$m = m_0 - 2.5(1 + \epsilon) \log_{10} S, \quad (2)$$

⁹ Most of these plates were identified by querying the Wide Field Plate Database, <http://www.skyarchive.org>

¹⁰ <http://archive.stsci.edu/dss/>

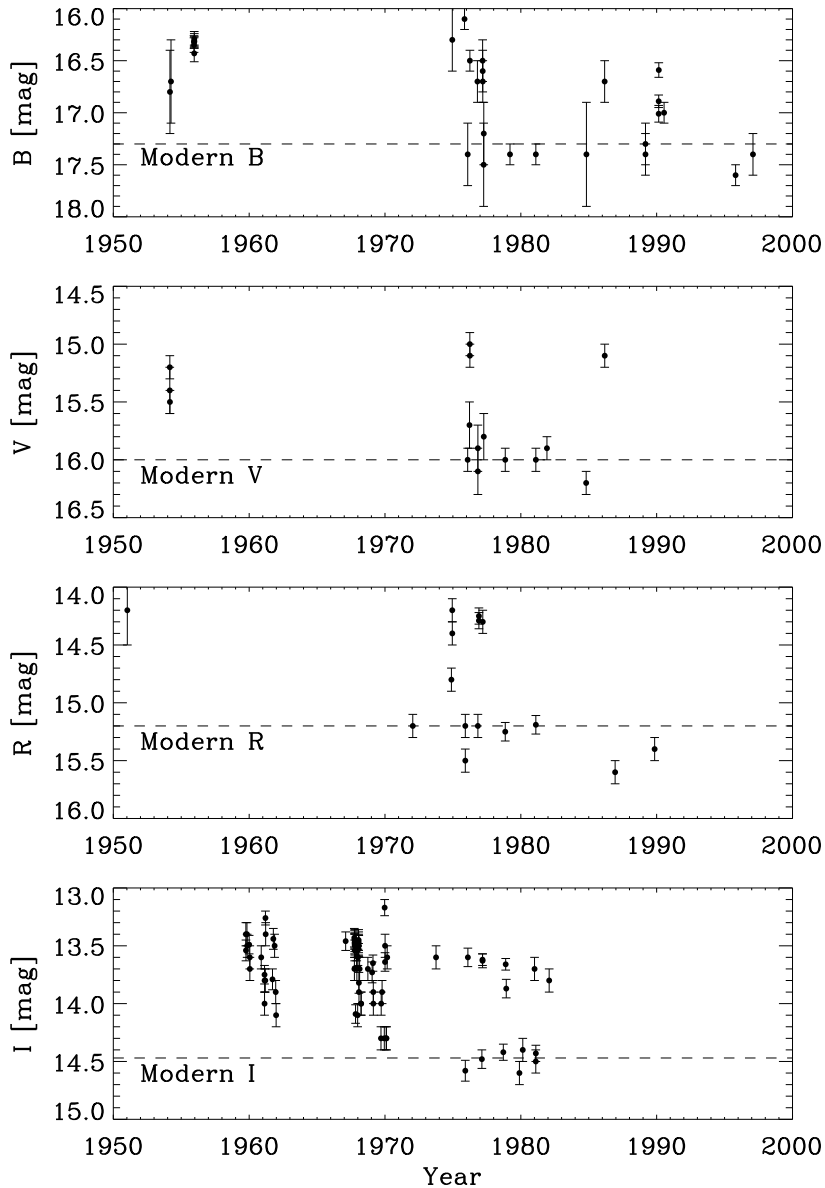


FIG. 1.— *BVRI* photometry of KH 15D over the last 5 decades derived from archival photographic plates.

where m is the apparent magnitude in the effective band pass produced by the emulsion and filter combination, and ϵ accounts for nonlinearity.

For each plate, we selected the band pass in the Johnson-Morgan-Cousins *UBVRI* system that is the closest match to the emulsion/filter combination that was employed (see Table 1). Then we estimated m_0 and ϵ for that plate using the set of 53 reference stars that we identified in Paper I. Those stars were selected by virtue of their proximity (they are all within a $20'$ box centered on KH 15D), their wide range of magnitudes and colors, and their relatively low level of variability. After measuring S for each of the reference stars, we found the values of m_0 and ϵ that minimize the sum of the squared residuals between Eqn. 2 and the magnitudes (in the appropriate band pass) measured by Flaccomio et al. (1999). In Paper I, we noted that higher order nonlinear terms and

color corrections were unhelpful in reducing the scatter in the magnitude relation. We found the same to be true for the present sample.

For almost all the plates, these steps were carried out by an automatic procedure, but there were a few plates that required individual attention. Two of the Tautenburg plates had an effective band pass approximating *U* band, but Flaccomio et al. (1999) did not measure *U* band magnitudes of our reference stars; for those plates, we used the $U - B$ measurements of Park et al. (2000). On the Mt. Wilson plates, there was a strong gradient in the background near KH 15D, due to the glare of the nearby B star; for those plates, we found it necessary to account for this gradient by fitting a first-order two-dimensional polynomial surface to the background. Finally, visual inspection of the POSSII IR plate revealed that KH 15D was much fainter than any of our

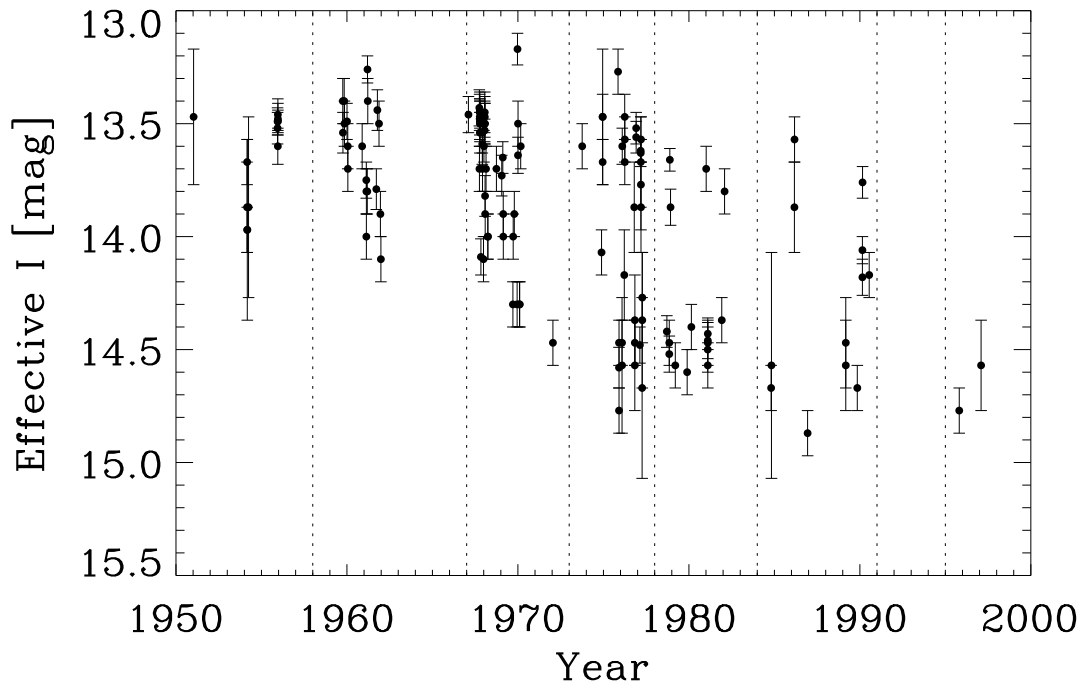


FIG. 2.— Effective I band photometric time series of KH 15D, based on the assumption that the system has always had the same color indices as the modern uneclipsed state.

reference stars. Rather than extrapolating to find the magnitude of KH 15D on this plate, we instead assign a firm lower limit of $I > 15.5$ based on the magnitude of the faintest of our reference stars.

3.1. Estimation of Errors

To estimate the uncertainty of each photometric measurement, we followed the same procedure as in Paper I. For each subset of plates obtained at the same telescope and with similar emulsion/filter combinations, we plotted the standard deviation in the resulting magnitudes of each star *versus* the mean magnitude of that star. The lower envelope of that relationship was taken to be the limiting uncertainty of our fitting procedure as a function of magnitude, $\sigma_{I,\min}(I)$. We also took into account the relative quality of each plate by computing σ_m , the scatter in the fit to Eqn. 2, and then we estimated the total uncertainty as

$$\text{Unc.} = \sigma_{I,\min}(I) \times \left(\frac{\sigma_m}{\sigma_{m,\min}} \right), \quad (3)$$

where $\sigma_{m,\min}$ is the minimum σ_m among all plates in that subset.

4. RESULTS

4.1. BVRI light curves

The magnitudes of KH 15D are given in Table 2. The first four columns give the Julian Date, the observatory (using the designations defined in Table 1), the closest corresponding $UBVRI$ band pass, and the apparent magnitude with the the corresponding estimated uncertainty. The light curves for each band pass are shown in Figure 1. For completeness, we have also plotted the measurements from Paper I.

The $BVRI$ light curves confirm two of the findings of Paper I: in the past, the system was formerly brighter and the fractional variations in total flux were smaller. The horizontal dashed lines in Figure 1 show the modern uneclipsed magnitudes of KH 15D. The light curves show that before about 1990, the system was often as much as 1 mag brighter than it appears today.

4.2. Test for chromatic variations

Hamilton et al. (2001) and Herbst et al. (2002) found that the flux variations that are observed today are nearly achromatic. Outside of eclipses, the $V - I$ and $V - R$ color indices do not vary by more than about 0.05 mag. Even during the 3 mag fading events, the system hardly changes color, although at minimum light it does appear to be systematically bluer by ≈ 0.1 mag in $V - R$. It would be interesting to know whether the flux variations in previous decades were also nearly achromatic, or whether they were accompanied by color changes.

The measurements reported in Paper I were almost all in I band. We considered only a few plates with different band passes, and only one pair of plates with different band passes (B and R) that were taken nearly simultaneously (on 1974 December 15). The result was $\Delta(B - R) = -0.14 \pm 0.30$, where $\Delta(B - R)$ is the difference between the $B - R$ index measured on that date, and the $B - R$ index of the modern uneclipsed state.

With the multi-band sample presented in this paper, we were able to test for color changes more extensively. There are 18 pairs of observations that took place within 2 days of each other and that have different effective band passes. For each of those pairs, Table 3 lists the mean Julian date and the measured color index, C . The third

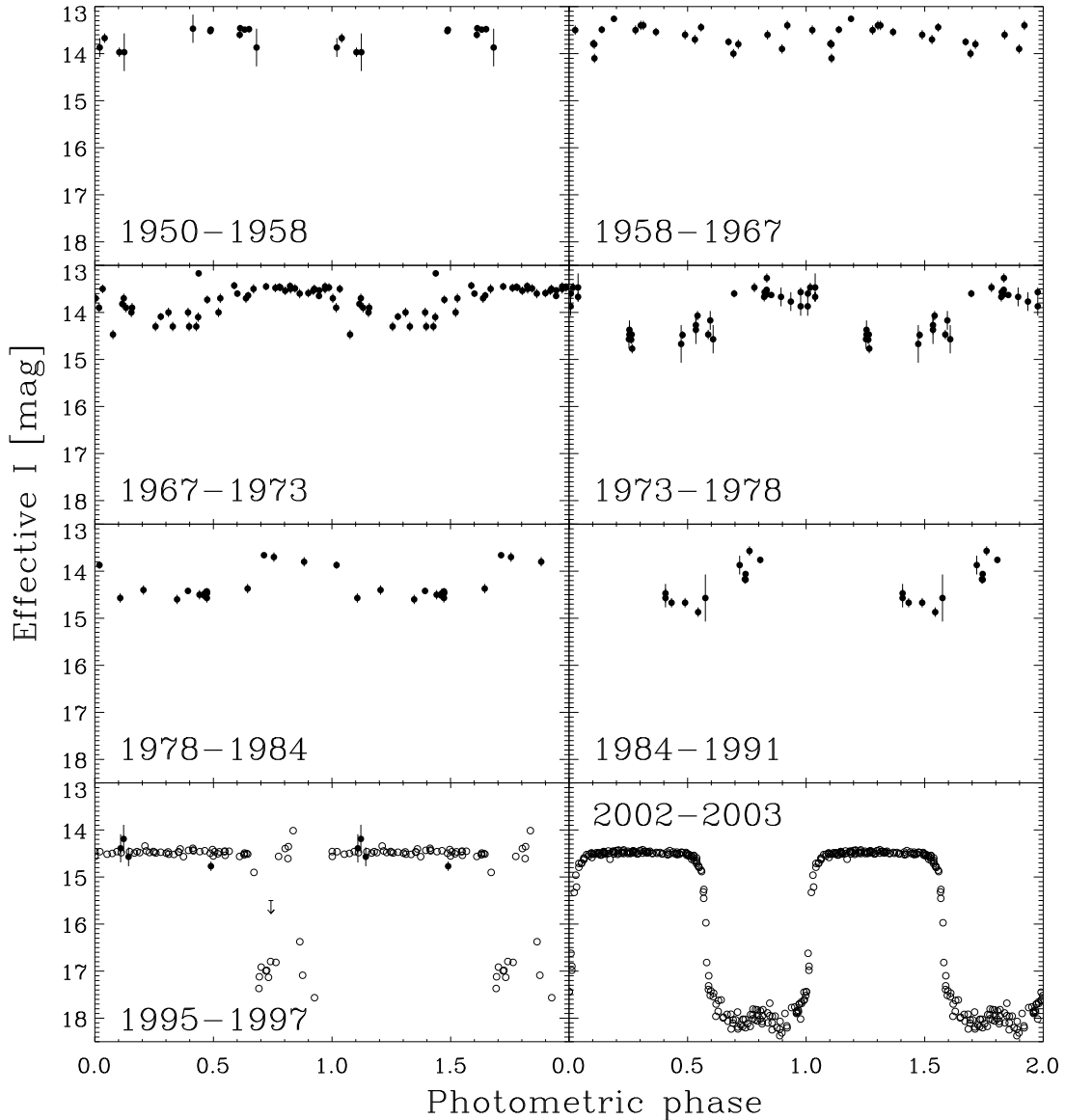


FIG. 3.— Phased light curves for different time periods. The filled circles are data based on the photographic plates described in this paper. The open circles (in the bottom panels) are modern CCD data, for which the error bars are smaller than the plot symbols.

column lists ΔC , which is the difference between C and the corresponding color index of the modern unclipped state¹¹. The final column gives the photometric phase, which is defined in § 4.4.

The result of this analysis is that there were no detectable color changes: all of the values of ΔC are consistent with zero, regardless of the photometric phase. Thus it appears as though the optical color indices of KH 15D have remained constant to within ≈ 0.2 mag over the past few decades.

¹¹ Here, for consistency, we have used the Flaccomio et al. (1999) values for the unclipped color indices. However, following Hamilton et al. (2001), we have assumed that the $B - V$ entry for KH 15D (star no. 391) in the catalog of Flaccomio et al. (1999) contains a typo, and should be 1.32 rather than 0.32. This makes the entry consistent with other published measurements (e.g. Park et al. 2000, who report $B - V = 1.308$) and with the color expected of a star of the observed K7 spectral class.

4.3. An “effective” I band time series

Under the assumption that the color indices have always been exactly constant, we can put all the measurements on the same magnitude scale. The last column of Table 2 gives the “effective” I -band magnitude, which was computed under the assumptions $U - I = 4.02$, $B - I = 2.94$, $V - I = 1.62$, and $R - I = 0.80$. This effective I band time series is shown in Figure 2.

4.4. Evolution of the light curve

We have divided the effective I band time series into different time intervals, bounded by the dotted lines in Figure 2, in order to examine how the time series has evolved over the past 5 decades. Since both the modern variations and the variations observed from 1967-1982 (Paper I) are nearly periodic, it is useful to plot the magnitude as a function of the photometric phase ϕ , which

is defined as

$$\phi = \frac{(\text{J.D.} - 2,434,800) \bmod P}{P}, \quad (4)$$

where $P = 48.38$ days is the orbital period that was determined by Johnson et al. (2004). We note that this definition of ϕ differs from the photometric phase that was used in Paper I, because of the updated period. In Figure 3 we have plotted phased light curves for each of the 6 time intervals covered by our data, along with phased light curves from CCD-based data that were kindly provided by W. Herbst and C. Hamilton.

The phased light curves clarify the nature of the photometric variations. From about 1965 to 1991, the system alternated between a bright state and a faint state with a 48-day period, just as the system does today. However, the modern bright state is approximately 1 mag fainter than the pre-1991 bright state. In fact, the modern bright state has approximately the same brightness as the pre-1991 *faint* state. The other striking feature of the phased light curves is that ϕ_{\min} , the phase corresponding to the midpoint of the faint state, has changed by nearly 0.5. Formerly it occurred at $\phi_{\min} \approx 0.32$. By 1995-96, it had shifted to $\phi_{\min} = 0.8$, although it is worth remembering that in that year and the few years to follow, the “faint state” included a short-lived rebrightening event.

These findings confirm and extend the results of Paper I, which were based almost entirely on the 1965-73 data. The enlarged sample indicates that the shallow, phase-shifted eclipses were occurring until at least 1991. It also shows that the variations were smaller and less regular in the years before 1965. Between 1958 and 1965, there is some evidence for a faint state centered at $\phi_{\min} \approx 0.7$, but the fractional variation appears to be $\lesssim 0.5$ mag, and the transition between the bright and faint states is more gradual. Before 1958, no particular pattern of variations is evident.

5. DISCUSSION

Winn et al. (2004) and Chiang & Murray-Clay (2004) hypothesized that KH 15D is a pair of stars in a mutual orbit with high eccentricity, and the “eclipses” are actually occultations by a circumbinary disk. A full analysis of this model should include all the available information, including the modern photometry, the photographic photometry, and the radial velocity measurements by Johnson et al. (2004). This will be the subject of a future paper. Here we simply describe how the basic properties of the light curves presented in this paper can be explained by the model, and point out one aspect of the new data that has not yet been explained.

In the model, we are viewing an eccentric binary system nearly edge-on. Today we can see only one of the two stars; we refer to the visible star as A, and the invisible one as B. The reason B is invisible is that its entire orbit is in the shadow of a circumbinary disk. Also shadowed is a portion of A’s orbit, near periapse. The 3 mag eclipses occur when A passes into the shadow, once per period. The reason for the decadal evolution of the light curve is that the line of nodes of the disk is regressing, in response to the gravitational torque produced by the stars. This causes the shadow of the disk

to sweep across the system. As a progressively larger portion of A’s orbit is shadowed, the eclipses increase in duration. Extrapolating backwards in time, star A used to be completely exposed, and only a portion of star B’s orbit (near apoapse) was shadowed. In that era, we observed periodic occultations of star B.

Thus, we interpret the historical light curve as follows. The periodic alternation between the bright and faint state is due to the periodic occultation of star B. The total flux was formerly larger, and the fractional variations were formerly smaller, because the steady light of star A was visible at all orbital phases. Finally, the reason for the phase shift is that the previous eclipses occurred around apoapse, whereas the modern eclipses occur around periapse.

Extrapolating even further backwards in time, one would expect to reach an era in which neither star was shadowed at any phase, and there were no photometric variations due to occultations. The new data presented in this paper show a somewhat more complicated picture. From 1951 to 1965, the system varied at the ≈ 0.5 mag level. This is certainly smaller than the 1 mag periodic variations observed between 1965 and 1991, but it is not zero. It is not clear whether these early variations were periodic, or erratic. The 1958-1965 data do seem to obey the 48-day periodicity, but the data are too sparse and the variations are too small to be certain.

In closing, we wish to note that although we have attempted to find as many useful photographic plates of NGC 2264 as possible, we do not claim that our collection is complete. Undoubtedly there are additional plates in other observatory archives. Additional photometry would be useful for a quantitative determination of the orbital parameters of the binary star and its putative circumbinary disk, especially if those data were taken during the years 1980-1995 where the time coverage of our light curves is not very complete.

We are indebted to Paolo Maffei, Gino Totsi, Yoshikazu Nakada, George Carlson, Steve Strom, Bill Schoening, Jean Mueller, Tony Misch, Peter Quinn, and Dave Monet for their kind assistance with the plate archives. We have enjoyed helpful conversations with Catrina Hamilton, Bill Herbst, Matt Holman, Geoff Marcy, and Fred Vrba about this work. M. Bagaglia is to be thanked for the digitization of part of the plates obtained by P. Maffei. We also thank Erin Johnson for assistance with the chromatic analysis and Liliana Lopez for help with the visual inspection of the Mt. Wilson plates. This work makes use of data from the digitized Italian photographic archives, produced under contract MIUR/COFIN 2002 to C. Barbieri, Department of Astronomy, University of Padova. J.N.W. is supported by NASA through Hubble Fellowship grant HST-HF-01180.02-A, awarded by the Space Telescope Science Institute, which is operated by the Association of Universities for Research in Astronomy, Inc., for NASA, under contract NAS 5-26555. M.T. acknowledges support from COST Action-283 and grant BNSF I-1103/2001 of the Bulgarian Ministry of Education and Science.

REFERENCES

- Agol, E., Barth, A. J., Wolf, S., & Charbonneau, D. 2004, *ApJ*, 600, 781
- Barbieri, C., Omizzolo, A., & Rampazzi, F. 2003, *Memorie della Societa Astronomica Italiana*, 74, 430
- Barge, P. & Viton, M. 2003, *ApJ*, 593, L117
- Barsunova, O. Y., Grinin, V. P., & Sergeev, S. G. 2004, *astro-ph/0409060*
- Brunzendorf, J. & Meusinger, H. 1999, *A&AS*, 139, 141
- Chiang, E. I. & Murray-Clay, R. A. 2004, *ApJ*, in press [*astro-ph/0312515*]
- Deming, D., Charbonneau, D., & Harrington, J. 2004, *ApJ*, 601, L87
- Flaccomio, E., Micela, G., Sciortino, S., Favata, F., Corbally, C., & Tomaney, A. 1999, *A&A*, 345, 521
- Grinin, V. P. & Tambovtseva, L. V. 2002, *Astronomy Letters*, 28, 601
- Hamilton, C. M., Herbst, W., Shih, C., & Ferro, A. J. 2001, *ApJ*, 554, L201
- Herbst, W., Hamilton, C. M., Vrba, F. J., Ibrahimov, M. A., Bailer-Jones, C. A. L., Mundt, R., Lamm, M., Mazeh, T., Webster, Z. T., Haisch, K. E., Williams, E. C., Rhodes, A. H., Balonek, T. J., Scholz, A., & Riffeser, A. 2002, *PASP*, 114, 1167
- Johnson, J. A., Marcy, G. W., Hamilton, C. M., Herbst, W., & Johns-Krull, C. M. 2004, *AJ*, 128, 1265
- Johnson, J. A. & Winn, J. N. 2004, *AJ*, 127, 2344
- Kearns, K. E. & Herbst, W. 1998, *AJ*, 116, 261
- Park, B., Sung, H., Bessell, M. S., & Kang, Y. H. 2000, *AJ*, 120, 894
- Stetson, P. B. 1979, *AJ*, 84, 1056
- Tokunaga, A. T., Dahm, S., Gässler, W., Hayano, Y., Hayashi, M., Iye, M., Kanzawa, T., Kobayashi, N., Kamata, Y., Minowa, Y., Nedachi, K., Oya, S., Pyo, T., Saint-Jacques, D., Terada, H., Takami, H., & Takato, N. 2004, *ApJ*, 601, L91
- Winn, J. N., Garnavich, P. M., Stanek, K. Z., & Sasselov, D. D. 2003, *ApJ*, 593, L121
- Winn, J. N., Holman, M. J., Johnson, J. A., Stanek, K. Z., & Garnavich, P. M. 2004, *ApJ*, 603, L45

TABLE 1
THE PLATE SAMPLE

Observatory (Designation)	Name of Telescope	Range of Years	Number of Plates	Filter	Emulsion	Approximate Band	Scanning Method
Asiago (ASI50)	40/50 cm Schmidt	1959-1969	20	RG5, RG665	I-N	I	Flatbed
Asiago (ASI120)	1.22 m Galilei	1955	6	none	103a-O	B	Flatbed
Kiso (KISO)	105/150 cm Kiso Schmidt	1975-1986	11	GG385	IIa-O	B	PDS
...	7	GG495	103a-D	V	...
...	4	GG495	IIa-D	V	...
...	1	RG610	103a-F	R	...
...	2	RG610	IIa-F	R	...
...	4	RG645	103a-E	R	...
...	6	RG695	I-N	I	...
Kitt Peak (KPNO)	4.0 m Mayall	1978-1981	2	RG610	IIIa-F	R	Flatbed
...	2	RG695	IV-N	I	...
...	1	GG385	IIIa-J	V	...
...	1	GG495	IIa-O	B	...
...	1	GG385	IIIa-J	B	...
Mt. Wilson (MTW)	60 in	1954	3	GG11	103a-D	V	Flatbed
...	2	GG13	103a-O	B	...
Palomar (POSS)	122/183 cm Oschin Schmidt	1951-1996	1	RP2444	103a-E	R	PMM
...	1	RG610	IIIa-F	R	...
...	1	RG9	IV-N	I	...
Rozhen NAO (ROZ)	2.0 m RCC	1990	4	GG385	ZU21	B	Flatbed
Tautenburg (TAU)	134/200 cm Schmidt	1972-1997	4	GG13	ZU	V	TPS
...	2	UG2	ZU	U	...
...	1	RG1	103a-E	R	...

TABLE 2
PHOTOMETRIC MEASUREMENTS OF KH 15D

Julian Date	Observatory	Band Pass	m [mag]	I_{eff} [mag] ^a
2433658.9	POSS	R	14.2 ± 0.4	13.4
2434801.0	MTW	V	15.4 ± 0.2	13.7
2434802.0	MTW	V	15.2 ± 0.2	13.5
2434805.0	MTW	V	15.5 ± 0.1	13.9
2434806.0	MTW	B	16.8 ± 0.4	13.9
2434833.0	MTW	B	16.7 ± 0.4	13.7
2435452.5	ASI120	B	16.35 ± 0.08	13.41
2435452.6	ASI120	B	16.32 ± 0.07	13.38
2435458.5	ASI120	B	16.43 ± 0.08	13.49
2435458.6	ASI120	B	16.29 ± 0.08	13.35
2435459.5	ASI120	B	16.32 ± 0.06	13.38
2435460.4	ASI120	B	16.31 ± 0.07	13.37
2436846.6	ASI040	I	13.4 ± 0.2	13.4
2436849.7	ASI040	I	13.5 ± 0.10	13.5
2436876.5	ASI040	I	13.4 ± 0.1	13.4
2436881.6	ASI040	I	13.5 ± 0.1	13.5
2436935.4	ASI040	I	13.49 ± 0.09	13.49
2436952.4	ASI040	I	13.6 ± 0.1	13.6
2436954.4	ASI040	I	13.7 ± 0.1	13.7
2437259.5	ASI040	I	13.6 ± 0.2	13.6
2437348.3	ASI040	I	13.75 ± 0.08	13.75
2437349.3	ASI040	I	14.0 ± 0.1	14.0
2437350.3	ASI040	I	13.8 ± 0.1	13.8
2437369.3	ASI040	I	13.8 ± 0.1	13.8
2437373.3	ASI040	I	13.26 ± 0.07	13.26
2437379.3	ASI040	I	13.4 ± 0.1	13.4
2437562.6	ASI040	I	13.8 ± 0.10	13.8
2437584.6	ASI040	I	13.44 ± 0.09	13.44
2437619.6	ASI040	I	13.5 ± 0.1	13.5
2437649.5	ASI040	I	13.9 ± 0.1	13.9
2437659.6	ASI040	I	14.1 ± 0.2	14.1
2440578.4	ASI040	I	13.17 ± 0.07	13.17
2441335.0	TAU	R	15.2 ± 0.1	14.4
2442726.3	KISO	B	16.1 ± 0.2	13.2
2442747.0	KISO	I	14.6 ± 0.10	14.6
2442747.1	KISO	R	15.2 ± 0.1	14.4
2442747.2	KISO	R	15.5 ± 0.1	14.7
2442811.1	KISO	V	16.0 ± 0.2	14.3
2442812.1	KISO	B	17.4 ± 0.3	14.5
2442859.9	KISO	V	15.7 ± 0.2	14.1
2442868.9	KISO	V	15.0 ± 0.1	13.4
2442870.9	KISO	B	16.5 ± 0.2	13.6
2442871.0	KISO	V	15.1 ± 0.1	13.5
2443073.3	KISO	B	16.7 ± 0.3	13.7
2443085.2	KISO	V	16.1 ± 0.2	14.5
2443085.3	KISO	V	15.9 ± 0.3	14.3
2443085.3	KISO	R	15.2 ± 0.1	14.4
2443113.2	KISO	R	14.29 ± 0.08	13.49
2443113.3	KISO	R	14.25 ± 0.08	13.45
2443192.9	KISO	I	14.48 ± 0.09	14.48
2443210.0	KISO	I	13.62 ± 0.05	13.62
2443211.0	KISO	I	13.63 ± 0.06	13.63
2443213.0	KISO	B	16.5 ± 0.2	13.5
2443215.0	KISO	B	16.6 ± 0.3	13.7
2443217.0	KISO	B	16.7 ± 0.3	13.7
2443217.0	KISO	R	14.3 ± 0.1	13.5
2443241.0	KISO	B	17.5 ± 0.4	14.5
2443244.0	KISO	B	17.2 ± 0.4	14.2
2443244.0	KISO	V	15.8 ± 0.2	14.1
2443769.3	KISO	I	14.42 ± 0.08	14.42
2443821.0	KPNO	R	15.25 ± 0.09	14.45
2443821.1	KISO	V	16.0 ± 0.1	14.4
2443833.2	KISO	I	13.66 ± 0.06	13.66
2443848.0	KPNO	I	13.87 ± 0.09	13.87
2443949.0	KPNO	B	17.4 ± 0.1	14.4
2444644.0	KPNO	V	16.0 ± 0.2	14.4
2444644.0	KPNO	R	15.19 ± 0.08	14.39
2444644.0	KPNO	I	14.43 ± 0.07	14.43
2444644.0	KPNO	B	17.4 ± 0.1	14.4
2444942.6	KISO	V	15.9 ± 0.2	14.2
2445996.7	KISO	V	16.2 ± 0.2	14.6
2446003.6	KISO	B	17.4 ± 0.6	14.5
2446494.4	KISO	B	16.7 ± 0.2	13.7
2446496.4	KISO	V	15.1 ± 0.1	13.5
2446776.2	KISO	R	15.6 ± 0.2	14.8
2447592.0	TAU	B	17.4 ± 0.2	14.5
2447592.0	TAU	B	17.3 ± 0.2	14.4
2447837.9	POSS	R	15.4 ± 0.2	14.6
2447947.0	ROZ	B	17.01 ± 0.08	14.07
2447947.0	ROZ	B	16.80 ± 0.07	13.95

TABLE 3
COLOR MEASUREMENTS OF KH15D

J.D.	Index	C	ΔC^a	ϕ^b
2434801.5	$B - V$	1.3 ± 0.2	0.0	0.03
2442747.0	$R - I$	0.6 ± 0.1	-0.1	0.26
2442747.0	$R - I$	0.9 ± 0.2	0.1	0.26
2442811.0	$B - V$	1.5 ± 0.2	0.2	0.58
2442870.0	$B - V$	1.5 ± 0.1	0.2	0.80
2442870.0	$B - V$	1.4 ± 0.1	0.1	0.80
2442871.0	$B - V$	1.6 ± 0.1	0.2	0.83
2443085.2	$V - R$	0.9 ± 0.2	0.1	0.25
2443085.2	$V - R$	0.7 ± 0.2	-0.1	0.25
2443212.0	$B - I$	2.8 ± 0.1	-0.1	0.87
2443217.0	$B - R$	2.4 ± 0.2	0.2	0.98
2443244.0	$B - V$	1.4 ± 0.2	0.1	0.53
2443821.0	$V - R$	0.9 ± 0.1	0.1	0.46
2444644.0	$B - V$	1.4 ± 0.2	0.1	0.47
2444644.0	$V - R$	0.8 ± 0.2	0.0	0.47
2444644.0	$R - I$	0.8 ± 0.1	0.0	0.47
2446495.5	$B - V$	1.5 ± 0.1	0.2	0.74
2450481.5	$U - B$	1.3 ± 0.4	0.2	0.13

^a $\Delta C \equiv C_{\text{measured}} - C_0$ where C_0 is the color index reported by Flaccomio et al. (1999) (or, in the case of the single $U - B$ entry, Park et al. (2000)).

^bBinary orbital phase, as defined in Eqn. 4.